ELSEVIER

Engineering Analysis with Boundary Elements 30 (2006) 882–896

ENGINEERING ANALYSIS with BOUNDARY ELEMENTS

www.elsevier.com/locate/enganabound

Regularized meshless method for multiply-connected-domain Laplace problems

K.H. Chen[a,*], J.H. Kao[b], J.T. Chen[b], D.L. Young[c], M.C. Lu[a]

[a]*Department of Information Management, Toko University, Chia-Yi 61363, Taiwan*
[b]*Department of Harbor and River Engineering, National Taiwan Ocean University, Keelung 20224, Taiwan*
[c]*Department of Civil Engineering and Hydrotech Research Institute, National Taiwan University, Taipei 10673, Taiwan*

Received 24 October 2005; accepted 14 June 2006

Abstract

In this paper, the regularized meshless method (RMM) is developed to solve two-dimensional Laplace problem with multiply-connected domain. The solution is represented by using the double-layer potential. The source points can be located on the physical boundary by using the proposed technique to regularize the singularity and hypersingularity of the kernel functions. The troublesome singularity in the traditional methods is avoided and the diagonal terms of influence matrices are easily determined. The accuracy and stability of the RMM are verified in numerical experiments of the Dirichlet, Neumann, and mixed-type problems under a domain having multiple holes. The method is found to perform pretty well in comparison with the boundary element method.

Keywords: Regularized meshless method; Subtracting and adding-back technique; Singularity; Hypersingularity; Multiply-connected problem; Method of fundamental solutions; Double-layer potential

1. Introduction

In recent years, science and engineering communities have paid much attention to the meshless method in which the element is free. Because of neither domain nor boundary meshing required for the meshless method, it is very attractive for engineers in modeling. Therefore, the meshless method becomes promising in solving engineering problems.

The boundary knot method (BKM) [1–5], boundary particle method [6] and method of fundamental solutions (MFS) [7–9] belong one kind of the boundary-discretization-type meshless methods. The BKM, developed in Ref. [4], uses the non-singular general solution to avoid the fictitious boundary outside the physical domain in the MFS. Consequently, the stability has greatly been improved, especially in handing multiply-connected problem in the BKM via the dual reciprocity method and the RBF as in the MFS. In particular, the BKM can produce the symmetric interpolation matrix which is often important in some problems (e.g., eigenvalue problem). The boundary particle method [6] is a truly boundary-only meshfree method for inhomogeneous problems, where the fundamental solution or the general solution is used to evaluate the homogeneous solution, while the high-order fundamental solution of the Laplace operator is employed to calculate the particular solution. The method can produce very accurate results with the boundary nodes for problems whose inhomogeneous function can be well represented by a polynomial approximation.

The MFS is attributed to Kupradze and Aleksidze [7] in 1964 and had been applied to potential [8], Helmholtz [10–12], diffusion [13], biharmonic [14] and elasticity problems [15]. In the MFS, the solution is approximated by a set of

*Corresponding author. Tel.: +886 5 3622889x821; fax: +886 5 3623916.
E-mail address: khc6177@mail.toko.edu.tw (K.H. Chen).

0955-7997/$ - see front matter © 2006 Elsevier Ltd. All rights reserved.
doi:10.1016/j.enganabound.2006.06.005

fundamental solutions of the governing equations which are expressed in terms of sources located outside the physical domain. The unknown coefficients in the linear combination of the fundamental solutions are determined by matching the boundary condition. The method is relatively easy to implement. It is adaptive in the sense that it can take into account sharp changes in the solution and in the geometry of the domain [16,17] and can easily incorporate complex boundary conditions [14]. A survey of the MFS and related method over the last 30 years can be found in Ref. [8]. However, the MFS is still not a popular method because of the debatable artificial boundary (fictitious boundary) distance of source location in numerical implementation especially for a complicated geometry. The diagonal coefficients of influence matrices are divergent in conventional case when the fictitious boundary approaches the physical boundary. Despite singularity-free merit, the influence matrices become severely ill posed when the fictitious boundary is far away from the physical boundary. It results in an ill-posed problem since the condition number of the influence matrix becomes very large.

Recently, Young et al. [18] developed a modified MFS, namely regularized meshless method (RMM), to overcome the drawback of MFS for solving the Laplace equation. The RMM eliminates the perplexing artificial boundary in the MFS, which can be arbitrary. The subtracting and adding-back technique [18–20] can regularize the singularity and hypersingularity of the kernel functions. This method can simultaneously distribute the observation and source points on the physical boundary even using the singular kernels instead of non-singular kernels [21,22]. The diagonal terms of the influence matrices can be extracted out by using the proposed technique.

Following the sources of [18] for simply-connected problems, this study makes the first attempt to extend the RMM to the multiply-connected-domain problems [23,24]. A general-purpose program is developed to solve the multiply-connected Laplace problems. The results will be compared with those of the BEM and analytical solutions. Furthermore, the sensitivity and convergence test will be studied through several examples to show the validity of our method.

2. Formulation

2.1. Governing equation and boundary conditions

Consider a boundary value problem with a potential $u(x)$, which satisfies the Laplace equation as follows:

$$\nabla^2 u(x) = 0, \quad x \in D, \tag{1}$$

subject to boundary conditions:

$$u(x) = \overline{u},\ x \in B_p^{\overline{u}}, \quad p = 1, 2, 3, \ldots, m, \tag{2}$$

$$t(x) = \overline{t},\ x \in B_q^{\overline{t}}, \quad q = 1, 2, 3, \ldots, m, \tag{3}$$

where ∇^2 is Laplacian operator, D is the domain of the problem, $t(x) = \partial u(x)/\partial n_{x_i}$, m is the total number of boundaries including $m-1$ numbers of inner boundaries and one outer boundary (the mth boundary), $B_p^{\overline{u}}$ is the essential boundary (Dirichlet boundary) of the pth boundary in which the potential is prescribed by $\overline{u}$ and $B_q^{\overline{t}}$ is the natural boundary (Neumann boundary) of the qth boundary in which the flux is prescribed by $\overline{t}$. Both $B_p^{\overline{u}}$ and $B_q^{\overline{t}}$ construct the whole boundary of the domain D as shown in Fig. 1(a).

2.2. Conventional MFS

By employing the RBF technique [3,25], the representation of the solution for multiply-connected problem as shown in Fig. 1(a) can be approximated in terms of the α_j strengths of the singularities at s_j as

$$u(x_i) = \sum_{j=1}^{N} T(s_j, x_i)\alpha_j = \sum_{j=1}^{N_1} T(s_j, x_i)\alpha_j + \sum_{j=N_1+1}^{N_1+N_2} T(s_j, x_i)\alpha_j, + \cdots + \sum_{j=N_1+N_2+\cdots+N_{m-1}+1}^{N} T(s_j, x_i)\alpha_j, \tag{4}$$

$$t(x_i) = \sum_{j=1}^{N} M(s_j, x_i)\alpha_j = \sum_{j=1}^{N_1} M(s_j, x_i)\alpha_j + \sum_{j=N_1+1}^{N_1+N_2} M(s_j, x_i)\alpha_j + \cdots + \sum_{j=N_1+N_2+\cdots+N_{m-1}+1}^{N} M(s_j, x_i)\alpha_j, \tag{5}$$

where x_i and s_j represent ith observation point and jth source point, respectively, α_j are the jth unknown coefficients (strength of the singularity), $N_1, N_2, \ldots, N_{m-1}$ are the numbers of source points on $m-1$ numbers of inner boundaries, respectively, N_m is the number of source points on the outer boundary, while N is the total numbers of source points ($N = N_1 + N_2 + \cdots + N_m$) and

$$M(s_j, x_i) = \frac{\partial T(s_j, x_i)}{\partial n_{x_i}}.$$

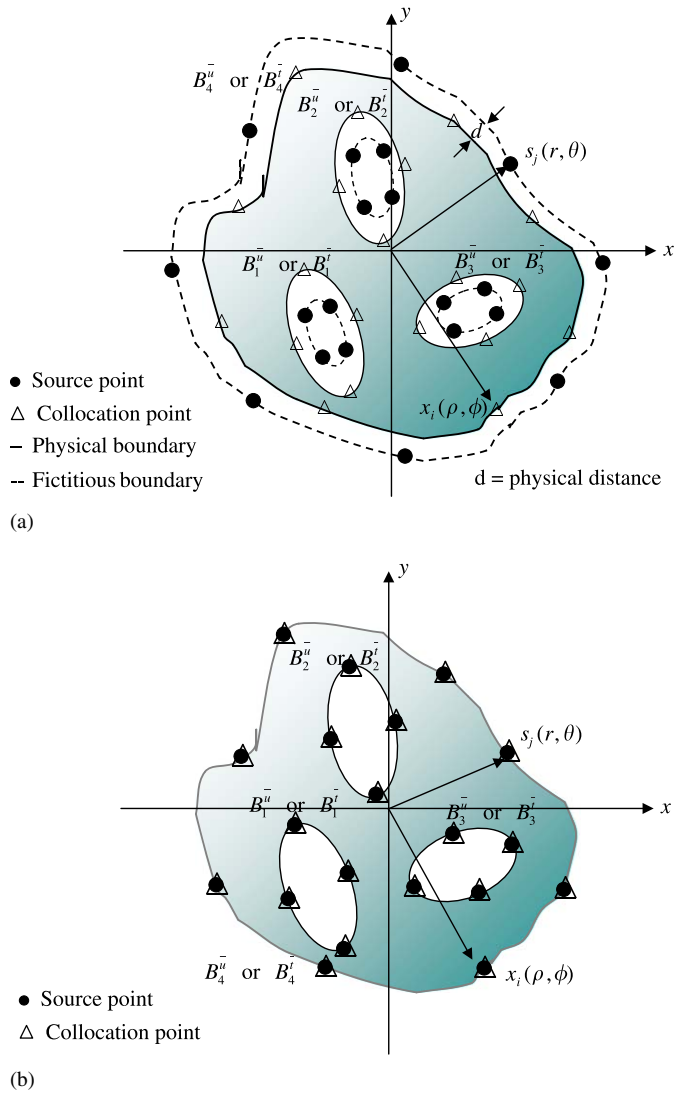

Fig. 1. The distribution of the source points and observation points and definition of r, θ, ρ, ϕ by using the conventional MFS and the RMM for the multiply-connected problems: (a) conventional MFS and (b) RMM.

After collocating N observation points to match with B.C., we can derive the unknown coefficient $\{\alpha_j\}_{j=1}^N$. The distributions of source points and observation points are shown in Fig. 1(a) for the MFS. The chosen bases are the double-layer potentials [18,21,22] as

$$T(s_j, x_i) = \frac{-\big((x_i - s_j), n_j\big)}{r_{ij}^2}, \tag{6}$$

$$M(s_j, x_i) = \frac{2\big((x_i - s_j), n_j\big)\big((x_i - s_j), \overline{n_i}\big)}{r_{ij}^4} - \frac{(n_j, \overline{n_i})}{r_{ij}^2}, \tag{7}$$

where (,) is the inner product of two vectors, r_{ij} is $|s_j - x_i|$, n_j is the normal vector at s_j, and $\bar{n}_i$ is the normal vector at x_i.

It is noted that the double-layer potentials have both singularity and hypersingularity at origin, which lead to the troublesome artificial boundary in the MFS. The fictitious distance between the fictitious (auxiliary) boundary (B') and the physical boundary (B), defined by d, shown in Fig. 1(a) needs to be chosen deliberately. To overcome the abovementioned shortcoming, s_j is distributed on the physical boundary, shown in Fig. 1(b), by using the proposed regularized technique as written in Section 2.3. The rationale for choosing double-layer potential instead of the single-layer potential as used in the RMM for the form of RBFs is to take the advantage of the regularization of the subtracting and adding-back technique, so that no fictitious distance is needed when evaluating the diagonal coefficients of influence matrices which will be explained in Section 2.4. The single-layer potential cannot be chosen because the following Eqs. (9), (12), (15) and (18) in Section 2.3 are not satisfied. If the single-layer potential is used, the regularization of subtracting and adding-back technique fails.

2.3. Regularized meshless method

When the collocation point x_i approaches the source point s_j, the potentials in Eqs. (4) and (5) become singular. Eqs. (4) and (5) for the multiply-connected problems need to be regularized by using the regularization of subtracting and adding-back technique [18–20] as follows:

$$u(x_i^{\mathrm{I}}) = \sum_{j=1}^{N_1} T(s_j^{\mathrm{I}}, x_i^{\mathrm{I}})\alpha_j + \cdots + \sum_{j=N_1+\cdots+N_{P-1}+1}^{N_1+\cdots+N_p} T(s_j^{\mathrm{I}}, x_i^{\mathrm{I}})\alpha_j + \cdots + \sum_{j=N_1+\cdots+N_{m-2}+1}^{N_1+\ldots+N_{m-1}} T(s_j^{\mathrm{I}}, x_i^{\mathrm{I}})\alpha_j + \sum_{j=N_1+\cdots+N_{m-1}+1}^{N} T(s_j^{\mathrm{O}}, x_i^{\mathrm{I}})\alpha_j - \sum_{j=N_1+\ldots+N_{P-1}+1}^{N_1+\cdots+N_p} T(s_j^{\mathrm{I}}, x_i^{\mathrm{I}})\alpha_i,\ x_i^{\mathrm{I}} \in B_p, \quad p = 1, 2, 3, \ldots, m-1, \tag{8}$$

where x_i^{I} is located on the inner boundary ($p = 1, 2, 3, \ldots, m-1$) and the superscript I and O denote the inward and outward normal vectors, respectively, and

$$\sum_{j=N_1+\cdots+N_{p-1}+1}^{N_1+\cdots+N_p} T(s_j^{\mathrm{I}}, x_i^{\mathrm{I}}) = 0,\ x_i^{\mathrm{I}} \in B_p, \quad p = 1, 2, 3, \ldots, m-1. \tag{9}$$

Therefore, we can obtain:

$$u(x_i^{\mathrm{I}}) = \sum_{j=1}^{N_1} T(s_j^{\mathrm{I}}, x_i^{\mathrm{I}})\alpha_j + \cdots + \sum_{j=N_1+\cdots+N_{p-1}+1}^{i-1} T(s_j^{\mathrm{I}}, x_i^{\mathrm{I}})\alpha_j + \sum_{j=i+1}^{N_1+\ldots+N_p} T(s_j^{\mathrm{I}}, x_i^{\mathrm{I}})\alpha_j + \ldots + \sum_{j=N_1+\cdots+N_{m-2}+1}^{N_1+\cdots+N_{m-1}} \times T(s_j^{\mathrm{I}}, x_i^{\mathrm{I}})\alpha_j + \sum_{j=N_1+\cdots+N_{m-1}+1}^{N} T(s_j^{\mathrm{O}}, x_i^{\mathrm{I}})\alpha_j - \left[\sum_{j=N_1+\cdots+N_{P-1}+1}^{N_1+\cdots+N_p} T(s_j^{\mathrm{I}}, x_i^{\mathrm{I}}) - T(s_i^{\mathrm{I}}, x_i^{\mathrm{I}})\right]\alpha_i,$$
$$x_i^{\mathrm{I}} \in B_p, \quad p = 1, 2, 3, \ldots, m-1. \tag{10}$$

When the observation point x_i^{O} locates on the outer boundary ($p = m$), Eq. (8) becomes

$$u(x_i^{\mathrm{O}}) = \sum_{j=1}^{N_1} T(s_j^{\mathrm{I}}, x_i^{\mathrm{O}})\alpha_j + \sum_{j=N_1+1}^{N_1+N_2} T(s_j^{\mathrm{I}}, x_i^{\mathrm{O}})\alpha_j + \cdots + \sum_{j=N_1+\cdots+N_{m-2}+1}^{N_1+\cdots+N_{m-1}} T(s_j^{\mathrm{I}}, x_i^{\mathrm{O}})\alpha_j + \sum_{j=N_1+\cdots+N_{m-1}+1}^{N} \times T(s_j^{\mathrm{O}}, x_i^{\mathrm{O}})\alpha_j - \sum_{j=N_1+\cdots+N_{m-1}+1}^{N} T(s_j^{\mathrm{I}}, x_i^{\mathrm{I}})\alpha_i, \quad x_i^{\mathrm{O\ and\ I}} \in B_p, \quad p = m, \tag{11}$$

where

$$\sum_{j=N_1+\cdots+N_{m-1}+1}^{N} T(s_j^{\mathrm{I}}, x_i^{\mathrm{I}})\alpha_i = 0,\ x_i^{\mathrm{I}} \in B_p, \quad p = m. \tag{12}$$

Hence, we obtain:

$$u(x_i^{\mathrm{O}}) = \sum_{j=1}^{N_1} T(s_j^{\mathrm{I}}, x_i^{\mathrm{O}})\alpha_j + \sum_{j=N_1+1}^{N_1+N_2} T(s_j^{\mathrm{I}}, x_i^{\mathrm{O}})\alpha_j + \ldots + \sum_{j=N_1+\cdots+N_{m-2}+1}^{N_1+\cdots+N_{m-1}} T(s_j^{\mathrm{I}}, x_i^{\mathrm{O}})\alpha_j + \sum_{j=N_1+\cdots+N_{m-1}+1}^{i-1} T(s_j^{\mathrm{O}}, x_i^{\mathrm{O}})\alpha_j + \sum_{j=i+1}^{N} T(s_j^{\mathrm{O}}, x_i^{\mathrm{O}})\alpha_j - \left[\sum_{j=N_1+\cdots+N_{m-1}+1}^{N} T(s_j^{\mathrm{I}}, x_i^{\mathrm{I}}) - T(s_i^{\mathrm{O}}, x_i^{\mathrm{O}})\right]\alpha_i, \quad x_i^{\mathrm{I\ and\ O}} \in B_p, \quad p = m. \tag{13}$$

Similarly, the boundary flux is obtained as

$$t(x_i^{\mathrm{I}}) = \sum_{j=1}^{N_1} M(s_j^{\mathrm{I}}, x_i^{\mathrm{I}})\alpha_j + \cdots + \sum_{j=N_1+\cdots+N_{p-1}+1}^{N_1+\cdots+N_p} M(s_j^{\mathrm{I}}, x_i^{\mathrm{I}})\alpha_j + \cdots + \sum_{j=N_1+\cdots+N_{m-2}+1}^{N_1+\cdots+N_{m-1}} M(s_j^{\mathrm{I}}, x_i^{\mathrm{I}})\alpha_j + \sum_{j=N_1+\cdots+N_{m-1}+1}^{N} M(s_j^{\mathrm{O}}, x_i^{\mathrm{I}})\alpha_j - \sum_{j=N_1+\cdots+N_{P-1}+1}^{N_1+\cdots+N_p} M(s_j^{\mathrm{I}}, x_i^{\mathrm{I}})\alpha_i,\ x_i^{\mathrm{I}} \in B_p, \quad p = 1, 2, 3, \ldots, m-1, \tag{14}$$

where

$$\sum_{j=N_1+\cdots+N_{p-1}+1}^{N_1+\cdots+N_p} M(s_j^{\mathrm{I}}, x_i^{\mathrm{I}}) = 0,\ x_i^{\mathrm{I}} \in B_p,\ p = 1, 2, 3, \ldots, m-1. \tag{15}$$

Therefore, we obtain:

$$\begin{aligned} t(x_i^{\mathrm{I}}) = & \sum_{j=1}^{N_1} M(s_j^{\mathrm{I}}, x_i^{\mathrm{I}})\alpha_j + \cdots + \sum_{j=N_1+\cdots+N_{p-1}+1}^{i-1} M(s_j^{\mathrm{I}}, x_i^{\mathrm{I}})\alpha_j + \sum_{j=i+1}^{N_1+\cdots+N_p} M(s_j^{\mathrm{I}}, x_i^{\mathrm{I}})\alpha_j \\ & + \ldots + \sum_{j=N_1+\cdots+N_{m-2}+1}^{N_1+\cdots+N_{m-1}} M(s_j^{\mathrm{I}}, x_i^{\mathrm{I}})\alpha_j + \sum_{j=N_1+\cdots+N_{m-1}+1}^{N} M(s_j^{\mathrm{O}}, x_i^{\mathrm{I}})\alpha_j \\ & - \left[\sum_{j=N_1+\cdots+N_{P-1}+1}^{N_1+\cdots+N_p} M(s_j^{\mathrm{I}}, x_i^{\mathrm{I}}) - M(s_i^{\mathrm{I}}, x_i^{\mathrm{I}})\right]\alpha_i,\ x_i^{\mathrm{I}} \in B_p, \quad p = 1, 2, 3, \ldots, m-1. \end{aligned} \tag{16}$$

When the observation point locates on the outer boundary ($p = m$), Eq. (14) yields

$$\begin{aligned} t(x_i^{\mathrm{O}}) = & \sum_{j=1}^{N_1} M(s_j^{\mathrm{I}}, x_i^{\mathrm{O}})\alpha_j + \sum_{j=N_1+1}^{N_1+N_2} M(s_j^{\mathrm{I}}, x_i^{\mathrm{O}})\alpha_j + \cdots + \sum_{j=N_1+\cdots+N_{m-2}+1}^{N_1+\cdots+N_{m-1}} M(s_j^{\mathrm{I}}, x_i^{\mathrm{O}})\alpha_j \\ & + \sum_{j=N_1+\cdots+N_{m-1}+1}^{N} M(s_j^{\mathrm{O}}, x_i^{\mathrm{O}})\alpha_j - \sum_{j=N_1+\cdots+N_{m-1}+1}^{N} M(s_j^{\mathrm{I}}, x_i^{\mathrm{I}})\alpha_i,\ x_i^{\mathrm{O\ and\ I}} \in B_p, \quad p = m. \end{aligned} \tag{17}$$

where

$$\sum_{j=N_1+\cdots+N_{m-1}+1}^{N} M(s_j^{\mathrm{I}}, x_i^{\mathrm{I}}) = 0,\ x_i^{\mathrm{I}} \in B_p, \quad p = m. \tag{18}$$

Hence, we obtain:

$$\begin{aligned} t(x_i^{\mathrm{O}}) = & \sum_{j=1}^{N_1} M(s_j^{\mathrm{I}}, x_i^{\mathrm{O}})\alpha_j + \sum_{j=N_1+1}^{N_1+N_2} M(s_j^{\mathrm{I}}, x_i^{\mathrm{O}})\alpha_j + \cdots + \sum_{j=N_1+\cdots+N_{m-2}+1}^{N_1+\cdots+N_{m-1}} M(s_j^{\mathrm{I}}, x_i^{\mathrm{O}})\alpha_j \\ & + \sum_{j=N_1+\cdots+N_{m-1}+1}^{i-1} M(s_j^{\mathrm{O}}, x_i^{\mathrm{O}})\alpha_j + \sum_{j=i+1}^{N} M(s_j^{\mathrm{O}}, x_i^{\mathrm{O}})\alpha_j - \left[\sum_{j=N_1+\cdots+N_{m-1}+1}^{N} M(s_j^{\mathrm{I}}, x_i^{\mathrm{I}}) - M(s_i^{\mathrm{O}}, x_i^{\mathrm{O}})\right]\alpha_i, \\ & x_i^{\mathrm{O\ and\ I}} \in B_p, \quad p = m. \end{aligned} \tag{19}$$

The detailed derivations of Eqs. (9), (12), (15) and (18) are given in the reference [18]. According to the dependence of the normal vectors for inner and outer boundaries [18], their relationships are:

$$\begin{cases} T(s_j^{\mathrm{I}}, x_i^{\mathrm{I}}) = -T(s_j^{\mathrm{O}}, x_i^{\mathrm{O}}), & i \neq j, \\ T(s_j^{\mathrm{I}}, x_i^{\mathrm{I}}) = T(s_j^{\mathrm{O}}, x_i^{\mathrm{O}}), & i = j, \end{cases} \tag{20}$$

$$\begin{cases} M(s_j^{\mathrm{I}}, x_i^{\mathrm{I}}) = M(s_j^{\mathrm{O}}, x_i^{\mathrm{O}}), & i \neq j, \\ M(s_j^{\mathrm{I}}, x_i^{\mathrm{I}}) = M(s_j^{\mathrm{O}}, x_i^{\mathrm{O}}), & i = j, \end{cases} \tag{21}$$

where the left and right hand sides of the equal sign in Eqs. (20) and (21) denote the kernels for observation and source point with the inward and outward normal vectors, respectively.

By using the proposed technique, the singular terms in Eqs. (4) and (5) have been transformed into regular terms:

$$\left(-\left[\sum_{j=N_1+N_2+\cdots+N_{P-1}+1}^{N_1+N_2+\cdots+N_p} T(s_j^{\mathrm{I}}, x_i^{\mathrm{I}}) - T(s_i^{\mathrm{I\ or\ O}}, x_i^{\mathrm{I\ or\ O}})\right]\right.$$

and

$$\left.-\left[\sum_{j=N_1+\cdots+N_{p-1}+1}^{N_1+\cdots+N_p} M(s_j^{\mathrm{I}}, x_i^{\mathrm{I}}) - M(s_i^{\mathrm{I\ or\ O}}, x_i^{\mathrm{I\ or\ O}})\right]\right)$$

in Eqs. (10), (13), (16) and (19), respectively, where $p = 1, 2, 3, \ldots, m$. The terms of

$$\sum_{j=N_1+\cdots+N_{P-1}+1}^{N_1+\cdots+N_p} T(s_j^{\mathrm{I}}, x_i^{\mathrm{I}})$$

and

$$\sum_{j=N_1+\cdots+N_{p-1}+1}^{N_1+\cdots+N_p} M(s_j^{\mathrm{I}}, x_i^{\mathrm{I}})$$

are the adding-back terms and the terms of $T(s_i^{\mathrm{I\ or\ O}}, x_i^{\mathrm{I\ or\ O}})$ and $M(s_i^{\mathrm{I\ or\ O}}, x_i^{\mathrm{I\ or\ O}})$ are the subtracting terms in the two brackets for regularization. After using the above-mentioned method of regularization of subtracting and adding-back technique [18–20], we are able to remove the singularity and hypersingularity of the kernel functions.

2.4. Derivation of influence matrices for arbitrary domain problems

By collocating N observation points to match with the BCs from Eqs. (10) and (13) for the Dirichlet problem, and the linear algebraic system is obtained:

$$\begin{Bmatrix} \begin{Bmatrix} \overline{u}_1 \\ \vdots \\ \overline{u}_{N_1} \end{Bmatrix} \\ \vdots \\ \begin{Bmatrix} \overline{u}_{N_1+N_2+\cdots+N_{m-1}+1} \\ \vdots \\ \overline{u}_N \end{Bmatrix} \end{Bmatrix}_{N\times 1} = \begin{bmatrix} [T_{11}]_{N_1\times N_1} & \cdots & [T_{1m}]_{N_1\times N_m} \\ \vdots & \ddots & \vdots \\ [T_{m1}]_{N_m\times N_1} & \cdots & [T_{mm}]_{N_m\times N_m} \end{bmatrix}_{N\times N} \begin{Bmatrix} \begin{Bmatrix} \alpha_1 \\ \vdots \\ \alpha_{N_1} \end{Bmatrix} \\ \vdots \\ \begin{Bmatrix} \alpha_{N_1+N_2+\cdots+N_{m-1}+1} \\ \vdots \\ \alpha_N \end{Bmatrix} \end{Bmatrix}_{N\times 1}, \tag{22}$$

where

$$[T_{11}] = \begin{bmatrix} -\left[\sum_{j=1}^{N_1} T(s_j^{\mathrm{I}}, x_1^{\mathrm{I}}) - T(s_1^{\mathrm{I}}, x_1^{\mathrm{I}})\right] & T(s_2^{\mathrm{I}}, x_1^{\mathrm{I}}) & \cdots & T(s_{N_1}^{\mathrm{I}}, x_1^{\mathrm{I}}) \\ T(s_1^{\mathrm{I}}, x_2^{\mathrm{I}}) & -\left[\sum_{j=1}^{N_1} T(s_j^{\mathrm{I}}, x_2^{\mathrm{I}}) - T(s_2^{\mathrm{I}}, x_2^{\mathrm{I}})\right] & \cdots & T(s_{N_1}^{\mathrm{I}}, x_2^{\mathrm{I}}) \\ \vdots & \vdots & \ddots & \vdots \\ T(s_1^{\mathrm{I}}, x_{N_1}^{\mathrm{I}}) & T(s_2^{\mathrm{I}}, x_{N_1}^{\mathrm{I}}) & \cdots & -\left[\sum_{j=1}^{N_1} T(s_j^{\mathrm{I}}, x_{N_1}^{\mathrm{I}}) - T(s_{N_1}^{\mathrm{I}}, x_{N_1}^{\mathrm{I}})\right] \end{bmatrix}_{N_1\times N_1}, \tag{23}$$

$$[T_{1m}] = \begin{bmatrix} T(s_{N_1+\cdots+N_{m-1}+1}^{\mathrm{O}}, x_1^{\mathrm{I}}) & T(s_{N_1+\cdots+N_{m-1}+2}^{\mathrm{O}}, x_1^{\mathrm{I}}) & \cdots & T(s_N^{\mathrm{O}}, x_1^{\mathrm{I}}) \\ T(s_{N_1+\cdots+N_{m-1}+1}^{\mathrm{O}}, x_2^{\mathrm{I}}) & T(s_{N_1+\cdots+N_{m-1}+2}^{\mathrm{O}}, x_2^{\mathrm{I}}) & \cdots & T(s_N^{\mathrm{O}}, x_2^{\mathrm{I}}) \\ \vdots & \vdots & \ddots & \vdots \\ T(s_{N_1+\cdots+N_{m-1}+1}^{\mathrm{O}}, x_{N_1}^{\mathrm{I}}) & T(s_{N_1+\cdots+N_{m-1}+2}^{\mathrm{O}}, x_{N_1}^{\mathrm{I}}) & \cdots & T(s_N^{\mathrm{O}}, x_{N_1}^{\mathrm{I}}) \end{bmatrix}_{N_1\times N_m}, \tag{24}$$

$$[T_{m1}] = \begin{bmatrix} T(s_1^{\mathrm{I}}, x^{\mathrm{O}}_{N_1+\cdots+N_{m-1}+1}) & T(s_2^{\mathrm{I}}, x^{\mathrm{O}}_{N_1+\cdots+N_{m-1}+1}) & \cdots & T(s^{\mathrm{I}}_{N_1}, x^{\mathrm{O}}_{N_1+\cdots+N_{m-1}+1}) \\ T(s_1^{\mathrm{I}}, x^{\mathrm{O}}_{N_1+\cdots+N_{m-1}+2}) & T(s_2^{\mathrm{I}}, x^{\mathrm{O}}_{N_1+\cdots+N_{m-1}+2}) & \cdots & T(s^{\mathrm{I}}_{N_1}, x^{\mathrm{O}}_{N_1+\cdots+N_{m-1}+2}) \\ \vdots & \vdots & \ddots & \vdots \\ T(s_1^{\mathrm{I}}, x^{\mathrm{O}}_{N}) & T(s_2^{\mathrm{I}}, x^{\mathrm{O}}_{N}) & \cdots & T(s^{\mathrm{I}}_{N_1}, x^{\mathrm{O}}_{N}) \end{bmatrix}_{N_m \times N_1}, \tag{25}$$

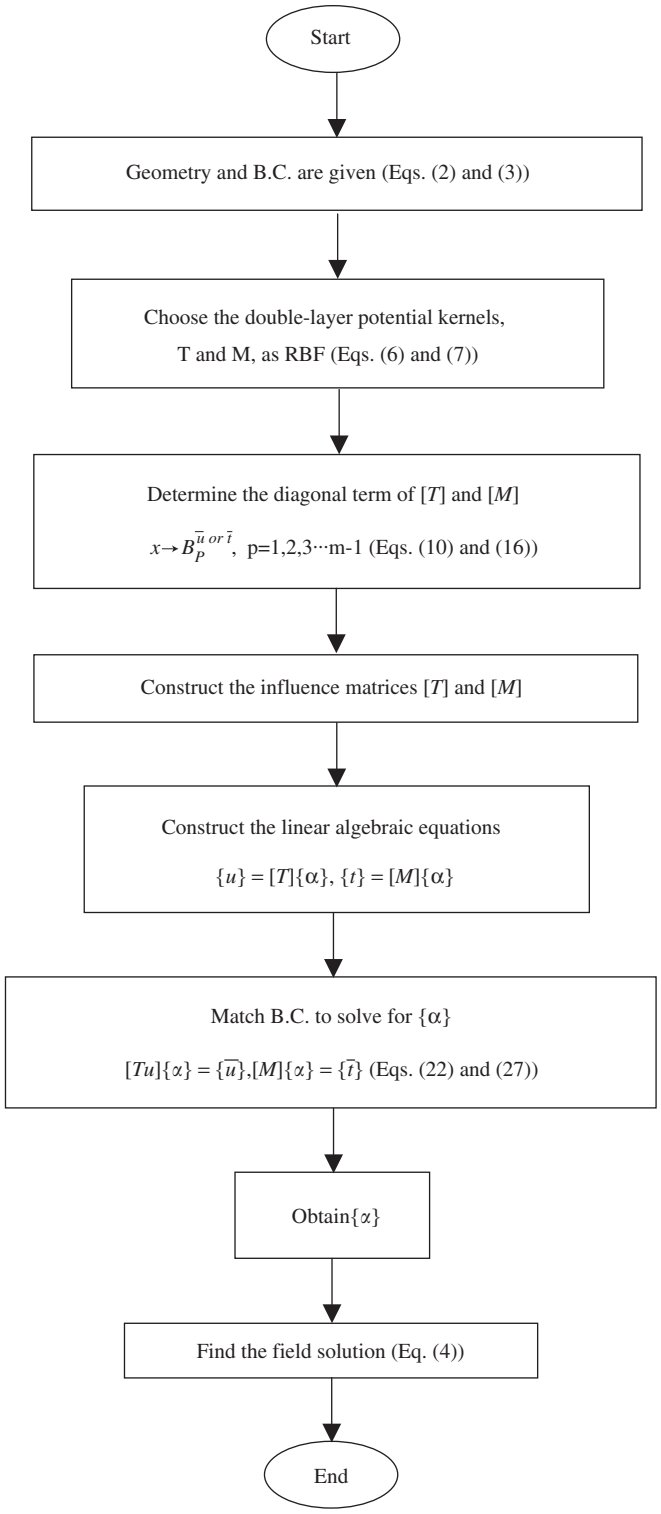

Fig. 2. Solution procedure.

$$[T_{mm}] = \begin{bmatrix} -\left[\sum_{j=N_1+\cdots+N_{m-1}+1}^{N} T(s_j^{\mathrm{I}}, x_{N_1+\cdots+N_{m-1}+1}^{\mathrm{I}}) - T(s_{N_1+\cdots+N_{m-1}+1}^{\mathrm{O}}, x_{N_1+\cdots+N_{m-1}+1}^{\mathrm{O}})\right] & \cdots & T(s_N^{\mathrm{O}}, x_{N_1+\cdots+N_{m-1}+1}^{\mathrm{O}}) \\ \vdots & \ddots & T(s_N^{\mathrm{O}}, x_{N_1+\cdots+N_{m-1}+2}^{\mathrm{O}}) \\ T(s_{N_1+\cdots+N_{m-1}+1}^{\mathrm{O}}, x_N^{\mathrm{O}}) & \cdots & -\left[\sum_{j=N_1+\cdots+N_{m-1}+1}^{N} T(s_j^{\mathrm{I}}, x_N^{\mathrm{I}}) - T(s_N^{\mathrm{O}}, x_N^{\mathrm{O}})\right] \end{bmatrix}_{N_m \times N_m} . \tag{26}$$

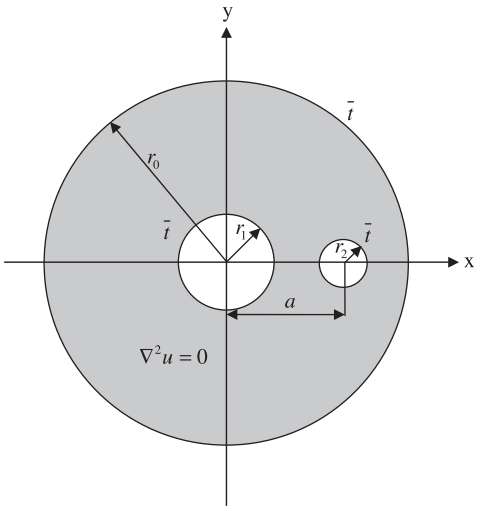

Fig. 3. Problem sketch for the case 1 ($r_0 = 2.0$, $r_1 = 0.5$, $r_2 = 0.25$ and $a = 1$).

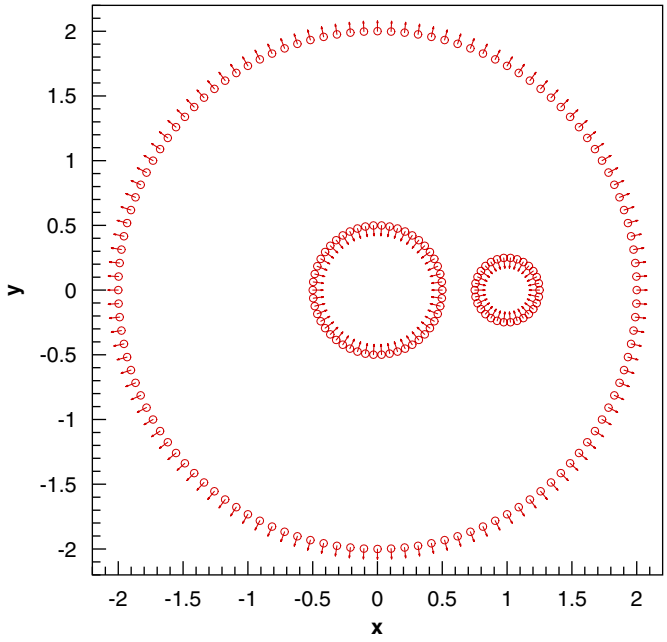

Fig. 4. Nodes distribution (200 nodes) for the case 1.

For the Neumann problem, Eqs. (16) and (19) yield

$$\begin{Bmatrix} \begin{Bmatrix} \bar{t}_1 \\ \vdots \\ \bar{t}_{N_1} \end{Bmatrix} \\ \vdots \\ \begin{Bmatrix} \bar{t}_{N_1+N_2+\cdots+N_{m-1}+1} \\ \vdots \\ \bar{t}_N \end{Bmatrix} \end{Bmatrix}_{N\times 1} = \begin{bmatrix} [M_{11}]_{N_1\times N_1} & \cdots & [M_{1m}]_{N_1\times N_m} \\ \vdots & \ddots & \vdots \\ [M_{m1}]_{N_m\times N_1} & \cdots & [M_{mm}]_{N_m\times N_m} \end{bmatrix}_{N\times N} \begin{Bmatrix} \begin{Bmatrix} \alpha_1 \\ \vdots \\ \alpha_{N_1} \end{Bmatrix} \\ \vdots \\ \begin{Bmatrix} \alpha_{N_1+N_2+\cdots+N_{m-1}+1} \\ \vdots \\ \alpha_N \end{Bmatrix} \end{Bmatrix}_{N\times 1}, \tag{27}$$

in which

$$[M_{11}] = \begin{bmatrix} -\left[\sum_{j=1}^{N_1} M(s_j^{\mathrm{I}}, x_1^{\mathrm{I}}) - M(s_1^{\mathrm{I}}, x_1^{\mathrm{I}})\right] & M(s_2^{\mathrm{I}}, x_1^{\mathrm{I}}) & \cdots & M(s_{N_1}^{\mathrm{I}}, x_1^{\mathrm{I}}) \\ M(s_1^{\mathrm{I}}, x_2^{\mathrm{I}}) & -\left[\sum_{j=1}^{N_1} M(s_j^{\mathrm{I}}, x_2^{\mathrm{I}}) - M(s_2^{\mathrm{I}}, x_2^{\mathrm{I}})\right] & \cdots & M(s_{N_1}^{\mathrm{I}}, x_2^{\mathrm{I}}) \\ \vdots & \vdots & \ddots & \vdots \\ M(s_1^{\mathrm{I}}, x_{N_1}^{\mathrm{I}}) & M(s_2^{\mathrm{I}}, x_{N_1}^{\mathrm{I}}) & \cdots & -\left[\sum_{j=1}^{N_1} M(s_j^{\mathrm{I}}, x_{N_1}^{\mathrm{I}}) - M(s_{N_1}^{\mathrm{I}}, x_{N_1}^{\mathrm{I}})\right] \end{bmatrix}_{N_1\times N_1}, \tag{28}$$

$$[M_{1m}] = \begin{bmatrix} M(s_{N_1+\cdots+N_{m-1}+1}^{\mathrm{O}}, x_1^{\mathrm{I}}) & M(s_{N_1+\cdots+N_{m-1}+2}^{\mathrm{O}}, x_1^{\mathrm{I}}) & \cdots & M(s_N^{\mathrm{O}}, x_1^{\mathrm{I}}) \\ M(s_{N_1+\cdots+N_{m-1}+1}^{\mathrm{O}}, x_2^{\mathrm{I}}) & M(s_{N_1+\cdots+N_{m-1}+2}^{\mathrm{O}}, x_2^{\mathrm{I}}) & \cdots & M(s_N^{\mathrm{O}}, x_2^{\mathrm{I}}) \\ \vdots & \vdots & \ddots & \vdots \\ M(s_{N_1+\cdots+N_{m-1}+1}^{\mathrm{O}}, x_{N_1}^{\mathrm{I}}) & M(s_{N_1+\cdots+N_{m-1}+2}^{\mathrm{O}}, x_{N_1}^{\mathrm{I}}) & \cdots & M(s_N^{\mathrm{O}}, x_{N_1}^{\mathrm{I}}) \end{bmatrix}_{N_1\times N_m}, \tag{29}$$

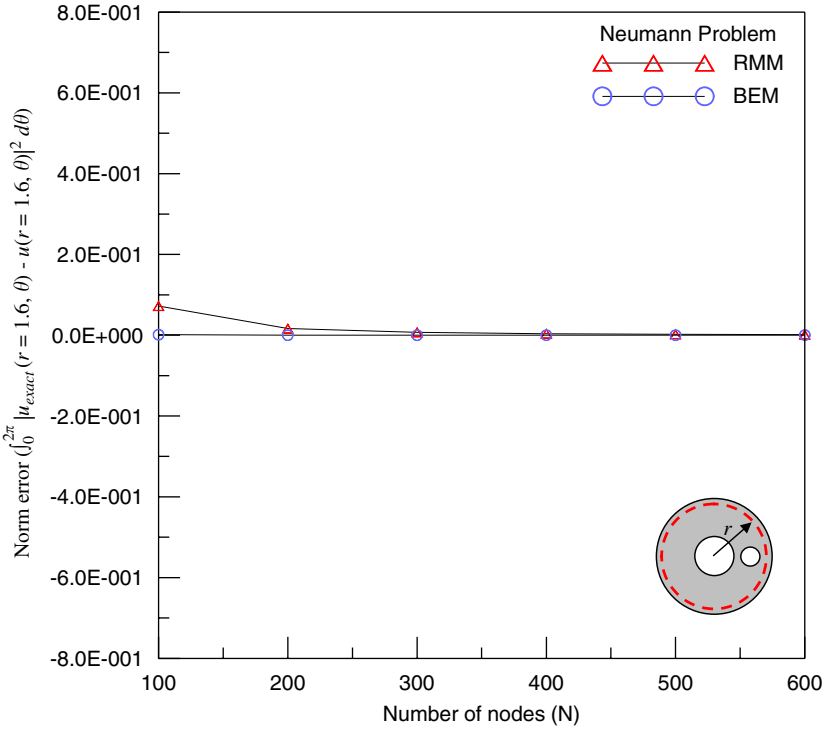

Fig. 5. The norm error along the radius $r = 1.6$ vs. the number of nodes for the case 1.

$$[M_{m1}] = \begin{bmatrix} M(s_1^{\mathrm{I}}, x_{N_1+\cdots+N_{m-1}+1}^{\mathrm{O}}) & M(s_2^{\mathrm{I}}, x_{N_1+\cdots+N_{m-1}+1}^{\mathrm{O}}) & \cdots & M(s_{N_1}^{\mathrm{I}}, x_{N_1+\cdots+N_{m-1}+1}^{\mathrm{O}}) \\ M(s_1^{I}, x_{N_1+\cdots+N_{m-1}+2}^{\mathrm{O}}) & M(s_2^{\mathrm{I}}, x_{N_1+\cdots+N_{m-1}+2}^{\mathrm{O}}) & \cdots & M(s_{N_1}^{\mathrm{I}}, x_{N_1+\cdots+N_{m-1}+2}^{\mathrm{O}}) \\ \vdots & \vdots & \ddots & \vdots \\ M(s_1^{\mathrm{I}}, x_N^{\mathrm{O}}) & M(s_2^{\mathrm{I}}, x_N^{\mathrm{O}}) & \cdots & M(s_{N_1}^{\mathrm{I}}, x_N^{\mathrm{O}}) \end{bmatrix}_{N_m \times N_1}, \tag{30}$$

$$[M_{mm}] = \begin{bmatrix} -\left[\sum_{j=N_1+\cdots+N_{m-1}+1}^{N} M(s_j^{\mathrm{I}}, x_{N_1+\cdots+N_{m-1}+1}^{\mathrm{I}}) - M(s_{N_1+\cdots+N_{m-1}+1}^{O}, x_{N_1+\cdots+N_{m-1}+1}^{O})\right] & \cdots & M(s_N^{\mathrm{O}}, x_{N_1+\cdots+N_{m-1}+1}^{\mathrm{O}}) \\ \vdots & \ddots & M(s_N^{\mathrm{O}}, x_{N_1+\cdots+N_{m-1}+2}^{\mathrm{O}}) \\ M(s_{N_1+\cdots+N_{m-1}+1}^{\mathrm{O}}, x_N^{\mathrm{O}}) & \cdots & -\left[\sum_{j=N_1+\cdots+N_{m-1}+1}^{N} M(s_j^{\mathrm{I}}, x_N^{\mathrm{I}}) - M(s_N^{\mathrm{O}}, x_N^{\mathrm{O}})\right] \end{bmatrix}_{N_m \times N_m}. \tag{31}$$

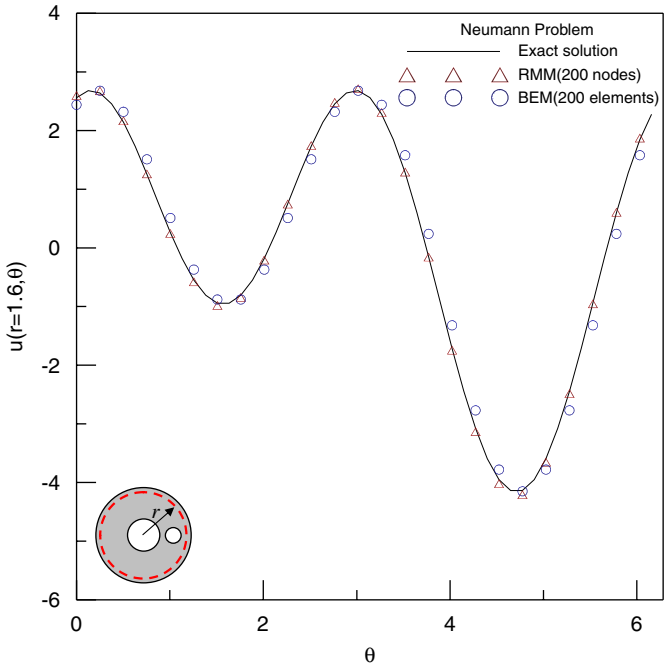

Fig. 6. The error analysis for the field solution along the radius $r = 1.6$ by using the RMM and BEM.

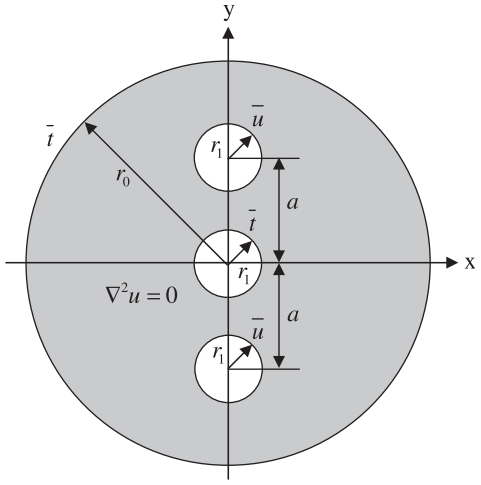

Fig. 7. Problem sketch for the case 2 ($r_0 = 2.0$, $r_1 = 0.25$ and $a = 1.0$).

For the mixed-type problem, a linear combination of Eqs. (22) and (27) is required to satisfy the mixed-type BCs. After the unknown density $\left(\{\alpha_j\}_{j=1}^{N}\right)$ are obtained by solving the linear algebraic equations, the field solution can be solved by using Eqs. (4) and (5). The solution procedure using the RMM is shown in Fig. 2.

3. Numerical examples

In order to show the accuracy and validity of the proposed method, the potential problems with multiply-connected domain subjected to the Dirichlet, Neumann and mixed-type BCs are considered.

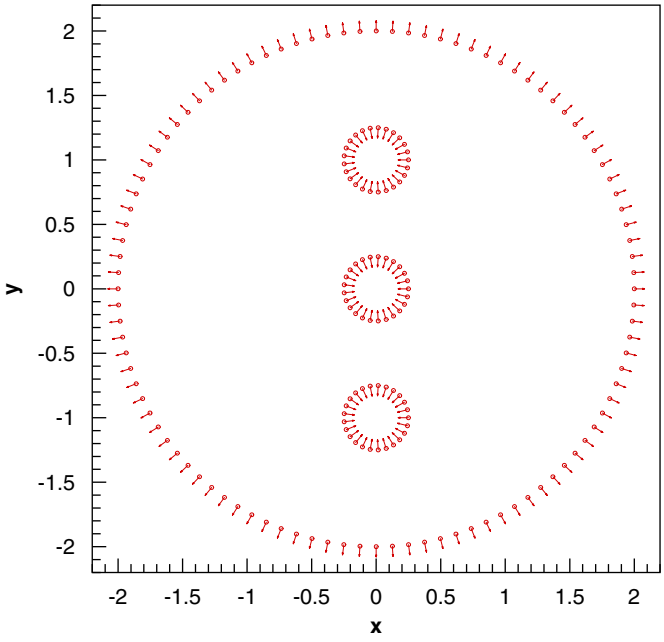

Fig. 8. Nodes distribution (175 nodes) for the case 2.

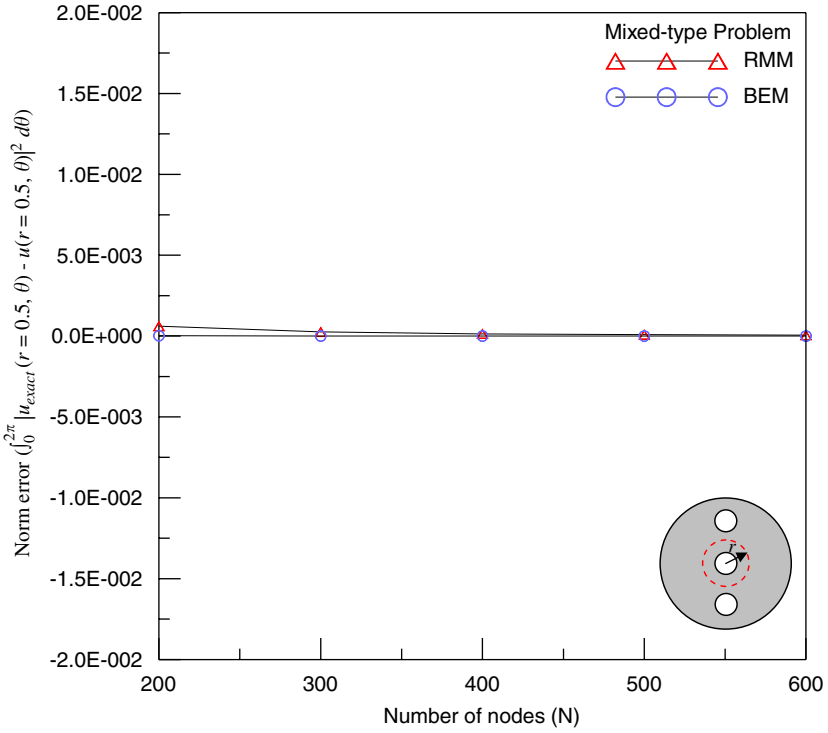

Fig. 9. The norm error along the radius $r = 0.5$ vs. the number of nodes for the case 2.

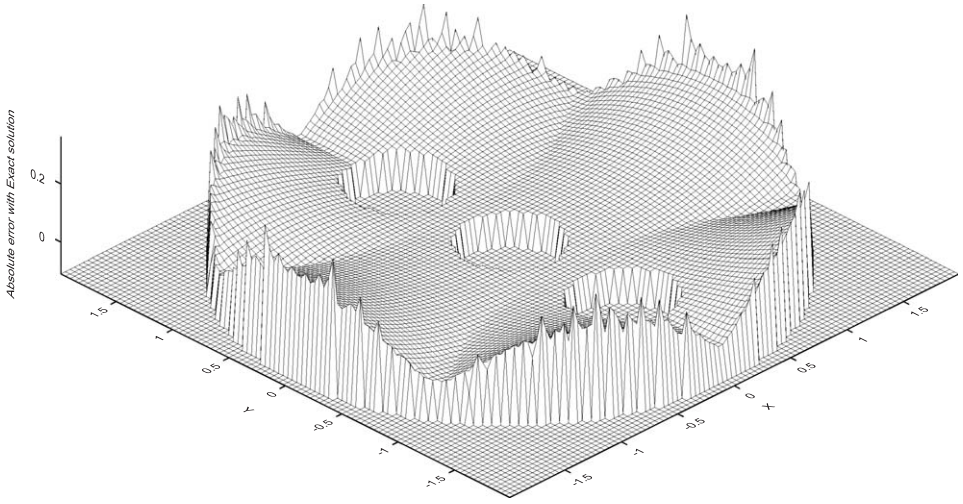

Fig. 10. Absolute error with the exact solution for the entire domain of case 2 (400 nodes).

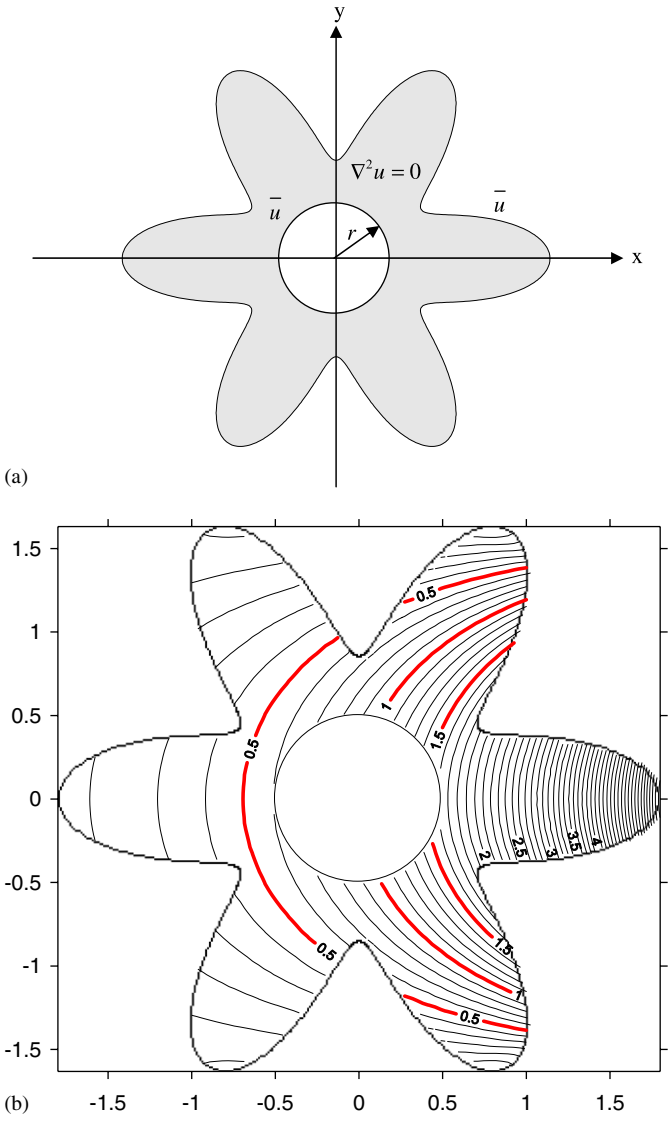

Fig. 11. Problem sketch and the exact solution for the case 3: (a) problem sketch and (b) field potential of the exact solution.

Case 1: Neumann problem.

The multiply-connected Neumann problem is shown in Fig. 3, and an analytical solution is

$$u = r^2 \cos(2\theta) + r \sin(\theta). \tag{32}$$

The nodes distribution (200 nodes) is shown in Fig. 4 and vector plot denotes the direction of out normal vector. To investigate the error analysis, the norm error is defined as

$$\int_0^{2\pi} \left| u_{\text{exact}}(r = 1.6, \theta) - u(r = 1.6, \theta) \right|^2 \mathrm{d}\theta.$$

The norm error vs. the total number N of source points is plotted in Fig. 5 by using the RMM and BEM, respectively. By collocating 200 boundary points, we can obtain the convergent result and the norm error is less than 10^{-2}. It is found that the data using BEM and present method agree very well when the number of nodes is over 400. The potentials along the radius $r = 1.6$ vs. angle are presented in Fig. 6 by using the RMM and the BEM, respectively. The RMM and BEM results perform pretty well in comparison with the exact solution.

Case 2: Mixed-type problem.

The mixed-type problem for multiply-connected domain is shown in Fig. 7, and an analytical solution is available as follows:

$$u = r^3 \cos(3\theta). \tag{33}$$

The nodes distribution (175 nodes) is shown in Fig. 8. The norm error is defined as $\int_0^{2\pi} \left| u_{\text{exact}}(r = 0.5, \theta) - u(r = 0.5, \theta) \right|^2 \mathrm{d}\theta$. The norm error of the RMM vs. the total number N of source points by using the RMM and the BEM, respectively, is shown in Fig. 9 and the convergent result is found after distributing 200 points. By adopting 200 boundary points, the norm error is less than 10^{-3}. The absolute errors of the RMM result (400 points) in the entire domain are plotted in Fig. 10.

Case 3: Arbitrary-shape problem.

The arbitrary-shape problem with continuous BCs is given in Fig. 11(a). An analytical solution is available as follows:

$$u = e^x \cos(y). \tag{34}$$

The field potential in Eq. (34) is shown in Fig. 11(b). The nodes distribution (200 nodes) is shown in Fig. 12. The norm error is defined as $\int_0^{2\pi} \left| u_{\text{exact}}(r = 0.9, \theta) - u(r = 0.9, \theta) \right|^2 \mathrm{d}\theta$. The norm error vs. the total number N of source points is shown in Fig. 13 and the convergent result can be found from Fig. 13.

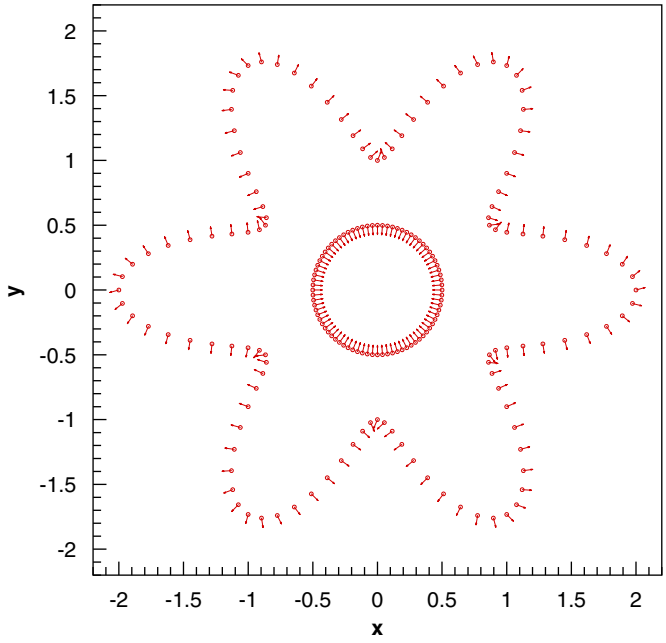

Fig. 12. Nodes distribution (200 nodes) for the case 3.

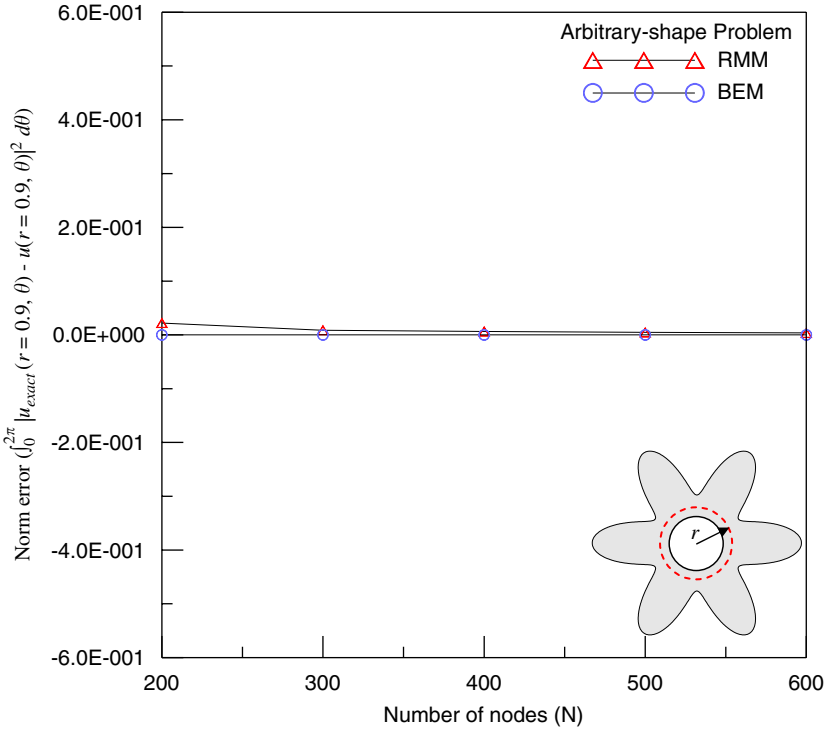

Fig. 13. The norm error along the radius $r = 0.9$ vs. the number of nodes for the case 3.

4. Conclusions

In this study, we use the RMM to solve the Laplace problems with multiply-connected domain subjected to the Dirichlet, Neumann and mixed-type BCs. Only the boundary nodes on the physical boundary are required. The perplexing fictitious boundary in the MFS is then circumvented. Despite the presence of singularity and hypersingularity of double-layer potential, the finite values of the diagonal terms of the influence matrix can be extracted out by employing subtracting and add-back techniques. The numerical results were obtained by applying the developed program to solve three problems with different BCs and shapes of domain. The convergent result is found from the convergent study in the three cases. Numerical results agreed very well with the analytical solutions and those of the BEM.

Acknowledgments

Financial support from the National Science Council under Grant no. NSC-94-2211-E-464-002 to the first author for Toko University is gratefully acknowledged.

References

[1] Hon YC, Chen W. Boundary knot method for 2D and 3D Helmholtz and the convection-diffusion problems with complicated geometry. Int J Numer Methods Eng 2003;56:1931–48.
[2] Chen W, Hon YC. Numerical investigation on convergence of boundary knot method in the analysis of homogeneous Helmholtz, modified Helmholtz, and convection–diffusion problems. Comput Methods Appl Mech Eng 2003;192:1859–75.
[3] Chen W, Tanaka M. A meshfree integration-free and boundary-only RBF technique. Comput Math Appl 2002;43:379–91.
[4] Chen W. Symmetric boundary knot method. Eng Anal Bound Elem 2002;26:489–94.
[5] Jin B, Chen W. Boundary knot method based on geodesic distance for anisotropic problems. J Comput Phys 2006;215:614–29.
[6] Chen W. Meshfree boundary particle method applied to Helmholtz problems. Eng Anal Bound Elem 2002;26:577–81.
[7] Kupradze VD, Aleksidze MA. The method of functional equations for the approximate solution of certain boundary value problems. USSR Comput Math Math Phys 1964;4:199–205.
[8] Fairweather G, Karageorghis A. The method of fundamental solutions for elliptic boundary value problems. Adv Comput Math 1998;9:69–95.
[9] Cheng AHD, Young DL, Tsai CC. The solution of Poisson's equation by iterative DRBEM using compactly supported, positive definite radial basis function. Eng Anal Bound Elem 2000;24:549–57.
[10] Young DL, Chen KH, Lee CW. Singular meshless method using double layer potentials for exterior acoustics. J Acoust Soc Am 2006;119:96–107.

[11] Karageorghis A. The method of fundamental solutions for the calculation of the eigenvalues of the Helmholtz equation. Appl Math Lett 2001;14:837–42.
[12] Chen JT, Chen IL, Lee YT. Eigensolutions of multiply connected membranes using the method of fundamental solutions. Eng Anal Bound Elem 2005;29:166–74.
[13] Chen CS, Golberg MA, Hon YC. The method of fundamental solutions and quasi-Monte-Carlo method for diffusion equations. Int J Numer Methods Eng 1998;43:1421–35.
[14] Poullikkas A, Karageorghis A, Georgiou G. Methods of fundamental solutions for harmonic and biharmonic boundary value problems. Comput Mech 1998;21:416–23.
[15] Cheng AHD, Chen CS, Golberg MA, Rashed YF. BEM for theromoelasticity and elasticity with body force: a revisit. Eng Anal Bound Elem 2001;25:377–87.
[16] Chen JT, Chen IL, Chen KH, Yeh YT, Lee YT. A meshless method for free vibration of arbitrarily shaped plates with clamped boundaries using radial basis function. Eng Anal Bound Elem 2004;28:535–45.
[17] Chen JT, Kuo SR, Chen KH, Cheng YC. Comments on vibration analysis of arbitrary shaped membranes using nondimensional dynamic influence function. J Sound Vib 2000;235:156–71.
[18] Young DL, Chen KH, Lee CW. Novel meshless method for solving the potential problems with arbitrary domain. J Comput Phys 2005;209:290–321.
[19] Hwang WS, Hung LP, Ko CH. Non-singular boundary integral formulations for plane interior potential problems. Int J Numer Methods Eng 2002;53:1751–62.
[20] Tournour MA, Atalla N. Efficient evaluation of the acoustic radiation using multipole expansion. Int J Numer Methods Eng 1999;46:825–37.
[21] Chen JT, Chang MH, Chen KH, Lin SR. The boundary collocation method with meshless concept for acoustic eigenanalysis of two-dimensional cavities using radial basis function. J Sound Vib 2002;257:667–711.
[22] Chen JT, Chang MH, Chen KH, Chen IL. Boundary collocation method for acoustic eigenanalysis of three-dimensional cavities using radial basis function. Comput Mech 2002;29:392–408.
[23] Baker GR, Shelley MJ. Boundary integral techniques for multi-connected domains. J Comput Phys 1986;64:112–32.
[24] Bird MD, Steele CR. A solution procedure for Laplace's equation on multiply-connected circular domain. ASME J Appl Mech 1992;59:398–404.
[25] Cheng AHD. Particular solutions of Laplacian, Helmholtz-type, and polyharmonic operators involving higher order radial basis functions. Eng Anal Bound Elem 2000;24:531–8.